

# A novel 3D infrared tomographic technology based on under-sampling and line-scanned structured heating <sup>†</sup>

Rongbang Wang <sup>1</sup>, Hai Zhang <sup>1,2,\*</sup> and Xavier Maldague <sup>2</sup>

<sup>1</sup> Center for Composite Materials and Structures (CCMS), Harbin Institute of Technology, 150001, Harbin, China; 22B918127@stu.hit.edu.cn

<sup>2</sup> Computer Vision and System Laboratory (CVSL), Department of Electrical and Computer Engineering, Laval University, G1V 0A6, Quebec City, Canada; Xavier.Maldague@gel.ulaval.ca

\* Correspondence: Hai.zhang@hit.edu.cn; Tel.: +86-13351104265

<sup>†</sup> Presented at the 18th International Workshop on Advanced Infrared Technology and Applications, Kobe, Japan, 15-19 September 2025.

**Abstract:** Traditional infrared thermography (IRT) techniques can only provide two-dimensional (2D) projections of surface temperatures, and it is difficult to intuitively present the surface profile of the three-dimensional (3D) structure and the spatial distribution of the internal defects. In this paper, a low cost, high efficiency and high precision photothermal 3D tomography technology was proposed by combining 3D thermography and infrared tomography for the first time. Specifically, this paper abandoned additional 3D sensors and complex motion systems such as robotic arms and scanning platforms. Differently, it utilized a galvanometer to deflect laser for line structure light scanning, and captured the thermal stripes generated on the structural surface using an infrared camera, and then realized the highly efficient 3D reconstruction; moreover, this work introduced undersampling strategy into photothermal coherence tomography (PCT) technology to enhance the ranging depth, and the ranging results were transmitted to the 3D coordinate system, so as to realize the photothermal 3D tomography. Through the detection experiments of metal additive manufacturing parts, it was shown that the proposed method could reconstruct the 3D contour of the specimen, and identified the first heterogeneous interface below the surface of the specimen.

**Keywords:** infrared thermography; 3D thermography; undersampling

## 1. Introduction

As an advanced non-destructive testing (NDT) method, laser thermography shows unique advantages in the detection of lack-of-fusion (LOF) defects in metal additive manufacturing (MAM) due to its non-contact and large-area imaging features [1-3]. However, in contrast to sound waves and electromagnetic waves that follow hyperbolic differential equations, thermal waves are essentially diffusive waves without wavefronts [4-6]. As a result, the traditional two-dimensional (2D) infrared thermography (IRT) can only capture the surface temperature distribution images that reflect the integral information along the axial depth, and it is difficult to quantitatively assess internal anomalies. Moreover, these 2D images are planar projections of three-dimensional (3D) objects, and cannot provide intuitive detection results for objects with complex geometries. With the rapid development of thermal science, modern control theory and computer vision in

Academic Editor: Firstname Lastname

Published: date

**Citation:** To be added by editorial staff during production.

**Copyright:** © 2025 by the authors. Submitted for possible open access publication under the terms and conditions of the Creative Commons Attribution (CC BY) license (<https://creativecommons.org/licenses/by/4.0/>).

recent years, it is possible to combine 3D imaging technology with quantitative infrared detection technology to realize photothermal 3D tomography.

In this paper, a low cost, and high accuracy photothermal 3D tomography method and system are proposed. The system first performs line structure light scanning by deflecting the laser using a galvanometer, and reconstructs the 3D surface contour of the specimen based on laser triangulation. Then, it enhances the depth measurement accuracy of photothermal coherence tomography (PCT) with the help of undersampling strategy, and projects the result into the 3D coordinate system, thus realizing the photothermal 3D tomography. With these advances, this work demonstrates photothermal 3D tomography results of MAM parts containing LOF defects, reconstructing the 3D surface contour of the specimen as well as the first subsurface heterogenous interface.

## 2. Materials and Methods

### 2.1. Specimen

To systematically evaluate the detection effectiveness of photothermal 3D tomography for MAM part, a 316L stainless steel blade simulated sample with a length of 130 mm, featuring variable width, variable thickness, and variable curvature, were selected for photothermal 3D tomography detection. The sample was processed using selective laser melting (SLM) forming technology, and its surface was sandblasted to remove burrs. The sample contains 9 circular LOF defects parallel to the surface, the diameters of the defects in the three columns from left to right along the projection direction are 8 mm, 9 mm, and 10 mm, while the depths of the defects in the three rows from top to bottom are 0.4 mm, 0.8 mm, and 1.2 mm, and the thickness of all defects is 0.5 mm.

### 2.2. Experimental Setup

The structure diagram of the photothermal 3D tomography system is shown in Fig. 1. The resolution of the Mid-wave infrared camera is  $640 \times 512$ , the integration time is 800  $\mu\text{s}$ , and the noise equivalent temperature difference is about 50 mK. The center wavelength of the laser is 1080 nm, the maximum output power is 400 W, and the switching optical response time  $\leq 10 \mu\text{s}$ . The key innovation of this paper is the linear structured optical galvanometer scanning photothermal 3D reconstruction technique, and the photothermal coherent tomography technique combined with undersampling strategy.

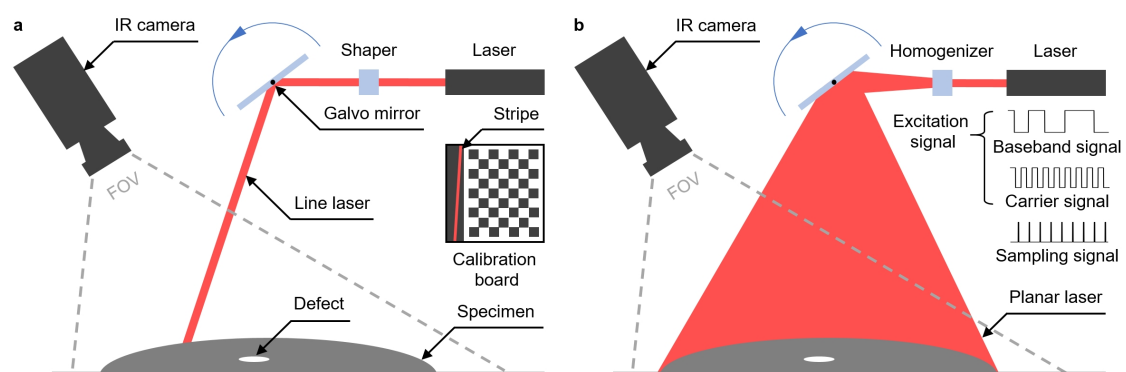


**Figure 1.** Structure diagram of the photothermal 3D tomography system: (a) linear structured light scanning 3D reconstruction; (b) PCT combined with undersampling strategy.

## 3. Results

As shown in Fig. 2b, the traditional long-pulse IRT technology detected 6 defects with depths of 0.4 mm and 0.8 mm, but when the depth of the preset defects reached 1.2

mm, the defects were almost unrecognizable. Due to the geometric distortion caused by the 2D projection imaging mechanism, the detection results could not truly present the curved surface characteristics of the sample. As shown in Fig. 2c, the photothermal 3D tomography detection method achieved accurate reconstruction of the 3D morphology of the blade simulated sample (the raised portion at the bottom of the sample was used for fixation and was not detected). The measured distance from the top to the bottom of the sample was 128 mm, and the measurement deviation  $\leq 1.2\%$ . The slice image shown in Fig. 2d clearly displays the curved surface characteristics of the blade simulated specimen at different positions and the depth of the pre-embedded defects: the detection results for the defects at depths of 0.4 mm and 0.8 mm are relatively clear, while the defect at a depth of 1.2 mm appears relatively fuzzy. Additionally, from Fig. 2d, the feature of the sample with thick edges and a thin center can also be observed. The two processes of 3D scanning and depth resolution took 2 s and 8 s, respectively. The sensor needs to be arranged only on one side of the sample, and the concave side of the imaging results is relatively smooth, without obvious artifacts or other significant noise interference.

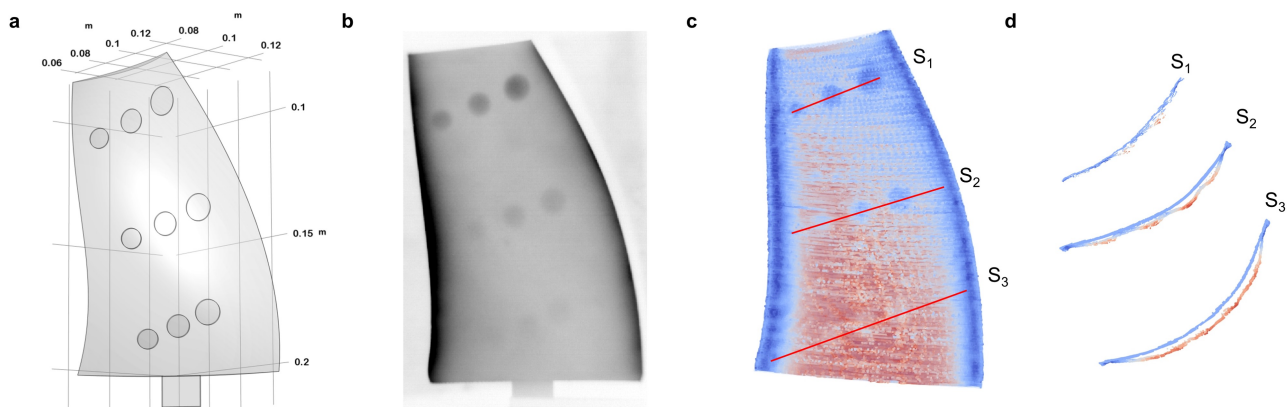


**Figure 2.** Detection results of 316L stainless steel blade simulated sample: (a) 3D schematic (the diameters of the defects in the three columns from left to right along the projection direction are 8 mm, 9 mm, and 10 mm, while the depths of the defects in the three rows from top to bottom are 0.4 mm, 0.8 mm, and 1.2 mm, and the thickness of all defects is 0.5 mm); (b) traditional 2D IRT detection; (c) photothermal 3D tomography with surface translucent treatment; (d) photothermal 3D tomography transaxial slice.

## 4. Discussion

In this paper, an innovative photothermal 3D tomography method and system are presented. Photothermal 3D tomography combines 3D IRT and infrared tomography technology to overcome the limitations of traditional detection methods in terms of hardware complexity, cost and detection performance. Instead of traditional 3D scanners and complex mechanical carrying parts, the method innovatively adopts galvanometer deflection laser to achieve linear structured light scanning, and captures thermal streaks generated by the excited structure surface through an infrared camera to achieve efficient 3D reconstruction. In addition, this paper also combines photothermal correlation technology with undersampling strategy to propose a new enhanced infrared tomography method, which can eliminate the interference caused by reflected laser on imaging results and weaken the problem of low contrast in defect areas caused by heat accumulation on the surface of specimens during laser irradiation. The experimental results show that the photothermal 3D tomography system can successfully recover the 3D contour of the surface of the MAM specimen, and there is no need to mark the key points and do not need to perform feature registration. The system was able to identify and recover the first

heterogeneous interface below the surface of the specimen, and this interface presented a clear boundary, unlike the progressive fuzzy boundary provided by traditional infrared tomography.

**Author Contributions:** Conceptualization, H.Z. and R.W.; methodology, R.W.; validation, R.W.; formal analysis, R.W.; investigation, R.W.; resources, X.M.; data curation, R.W.; writing—original draft preparation, R.W.; writing—review and editing, H.Z. and R.W.; visualization, R.W.; supervision, H.Z.; project administration, X.M.; funding acquisition, H.Z. All authors have read and agreed to the published version of the manuscript.

**Funding:** This work was supported by the National Key R&D Program of China (Grant No. 2023YFE0197800).

**Institutional Review Board Statement:** Not applicable.

**Informed Consent Statement:** Informed consent was obtained from all subjects involved in the study.

**Data Availability Statement:** The data are available on request to the corresponding author.

**Conflicts of Interest:** The authors declare no conflict of interest.

## References

- Deng, B.; Wu, W.; Li, X.; Wang, H.; He, Y.; Shen, G.; Tang, Y.; Zhou, K.; Zhang, Z.; Wang, Y. Active 3-D Thermography Based on Feature-Free Registration of Thermogram Sequence and 3-D Shape Via a Single Thermal Camera. *IEEE Trans. Ind. Electron.* 2022, 69, 11774–11784. <https://doi.org/10.1109/TIE.2021.3120471>
- Wang, R.; Pei, C.; Xia, R.; Wang, Q.; Chen, Z. A Portable Fiber Laser Thermography System With Beam Homogenizing for CFRP Inspection. *NDT & E Int.* 2021, 124, 102550. <https://doi.org/10.1016/j.ndteint.2021.102550>
- Zhang, H.; Sfarra, S.; Sarasini, F.; Ibarra-Castanedo, C.; Perilli, S.; Fernandes, H.; Duan, Y.; Peeters, J.; Avdelidis, N.P.; Maldague, X. Optical and Mechanical Excitation Thermography for Impact Response in Basalt-Carbon Hybrid Fiber-Reinforced Composite Laminates. *IEEE Trans. Ind. Inform.* 2018, 14, 514–522. <https://doi.org/10.1109/TII.2017.2744179>
- Kaiplavil, S.; Mandelis, A. Truncated-Correlation Photothermal Coherence Tomography for Deep Subsurface Analysis. *Nat. Photonics*, 2014, 8, 635–642. <https://doi.org/10.1038/nphoton.2014.111>
- Wang, F.; Wang, Y.; Liu, J.; Wang, Yang. The Feature Recognition of CFRP Subsurface Defects Using Low-Energy Chirp-Pulsed Radar Thermography. *IEEE Trans. Ind. Inform.* 2020, 16, 5160–5168. <https://doi.org/10.1109/TII.2019.2954718>
- Zhu, P.; Wang, R.; Sivagurunathan, K.; Sfarra, S.; Sarasini, F.; Ibarra-Castanedo, C.; Maldague, X.; Zhang, H.; Mandelis, A. Frequency multiplexed photothermal correlation tomography for non-destructive evaluation of manufactured materials. *Int. J. Extreme Manuf.* 2025, 7, 035601. <https://doi.org/10.1088/2631-7990/ada837>

**Disclaimer/Publisher's Note:** The statements, opinions and data contained in all publications are solely those of the individual author(s) and contributor(s) and not of MDPI and/or the editor(s). MDPI and/or the editor(s) disclaim responsibility for any injury to people or property resulting from any ideas, methods, instructions or products referred to in the content.